Particle & Particle Systems Characterization
www.particle-journal.com



# Strengthening and Stiffening Graphene Oxide Fiber with Trivalent Metal Ion Binders

*Wonsik Eom, Hun Park, Sung Hyun Noh, Ki Hwan Koh, Kichun Lee, Won Jun Lee,* and Tae Hee Han**

Liquid crystalline graphene oxide (LC-GO) is of widespread interest from fundamental and applied perspectives because of its intrinsic fluidic nature and structural alignment effect.[1,2] As noted, colloidal liquid crystal is the structured fluid state of anisotropic shaped colloids possessing liquid-like fluidity as well as crystal-like ordering.[3] Highly concentrated colloids of graphene oxide (GO) have shown interesting phenomena, such as lateral alignment induced assembly behavior.[4] These observations have stimulated interest for the macroscopic assembly of GO to form fibers since they are stable and of well-arranged order readily.[5–7] Production of GO fiber is analogous to methods used for producing high performance synthetic fiber (e.g., aramid), with the transformation of a LC solution into a solid filament, which is achieved by the addition of salts.[8,9] However, the first experimental realization of GO fiber via wet spinning, has not come to fruition in terms of mechanical performance.[10] This is due to the challenging nature of controlling the microstructure of GO flakes, resulting in unsaturated interactions during coagulation.[11] Poor interaction between GO flakes and the insufficient salts for coagulation hinders the realization of performance fibers.[12] Therefore, pathways to efficiently clot GO colloids into fibers with salt should be considered.

So far, the greatest challenge is to maintain the structural integrity of GO flakes during the coagulation process. Utilizing multivalent ion has emerged as an initial candidate to relieve this issue.[6,13–15] A good alternative is to use specific divalent metal ions, for example, $Cu^{2+}$ and $Ca^{2+}$ ions.[5–7,16] Carboxyl, hydroxyl, epoxy groups are abundant on GO, allowing coordinate bonds with $Cu^{2+}$ and $Ca^{2+}$, which lead to much higher mechanical strength fibers than when utilizing monovalent ions.[6] A range of divalent metal cations have been used to enhance mechanical strength, for example, $Ca^{2+}$ ($\sigma$ = 412 MPa, $E$ = 20.1 GPa)[6] and $Cu^{2+}$ ($\sigma$ = 274.3 MPa, $E$ = 6.4 GPa),[7] however, their mechanical performance is limited compared to commercial carbon fibers. Here, we present a straightforward fabrication method to produce GO fibers with LC solution of GO using trivalent cation salts as an ionic binder. To utilize the full potential of GO fiber, it is critically important to control the microstructure of fiber. The microstructure of GO fibers, such as shape and *d*-spacing between sheets, is ultimately controlled by the metal cation coagulants which are then processed into a fiber. Given the advantages of LC-GO, the resulting microstructure dominates most of the fiber mechanical properties (stiffness, strength, strain, etc.), and consequently its control in the early stage is regarded as a key method to achieve high mechanical performance. The underlying advantage is that trivalent metal cations modulate chemical interactions between GO sheets and drive ion cross-linking, which improves mechanical properties remarkably.

To see the effect of GO coagulation with multivalent cation binders, $Co^{2+}$, $Al^{3+}$, and $Fe^{3+}$ were considered. Well dispersed GO was prepared as described in the Experimental Section and was observed by atomic force microscopy (AFM) topography and the thickness of GO sheets were measured as 1.2 nm (**Figure 1**a). GO aqueous dispersions were prepared by dispersing GO powders in deionized water (DIW) by mild sonication (Figure 1b). Dispersed GO solutions (1.0 mg $mL^{-1}$) were kept stationary between two crossed polarizers and their LC phases were characterized with the observation of the textures of nematic LC. As presented in Figure 1c, GO dispersion showed the optical birefringence morphology; dark and bright brushes were interwoven, signifying a nematic LC phase. This phase implies that the anisotropic particles are well dispersed within the dispersing media without aggregates, which is largely resulted from electrostatic repulsion.[1,17–19] To observe the changes of LC-GO in the presence of cations, different metal salts were added at a concentration of $20 \times 10^{-3}$ M. The addition of cations eventually disrupted dense LC patterns. Interestingly, it was still possible to observe the birefringence effect. This observation indicates that the multivalent cation acts as an ionic binder for the GO and the dispersion formed stacked crystalline-like GO sheets.

The prepared GO dispersions were spun and the dispersions gelated in the coagulation bath. The cations which diffuse into the inner structure of the GO gel undergo electrostatic attraction with the negative charge of GO's oxygen functional groups, leading to bonding in the basal planes.[20] Furthermore, the coordination bonds between the GO and metal cations act as bridges between the sheet edges.[21–23] The GO gels immobilized by cation binder are pulled out of the coagulation bath and continuously coiled along the reel. Drafting was not performed

W. Eom, H. Park, S. H. Noh, K. H. Koh, Prof. T. H. Han
Department of Organic and Nano Engineering
Hanyang University
Seoul 04763, Republic of Korea
E-mail: than@hanyang.ac.kr
Prof. K. Lee
Department of Industrial Engineering
Hanyang University
Seoul 04763, Republic of Korea
Dr. W. J. Lee
Department of Chemistry
Imperial College London
London SW7 2AZ, UK
E-mail: wonjun.lee@imperial.ac.uk

**DOI: 10.1002/ppsc.201600401**

  

Particle
& Particle Systems Characterization
www.particle-journal.com



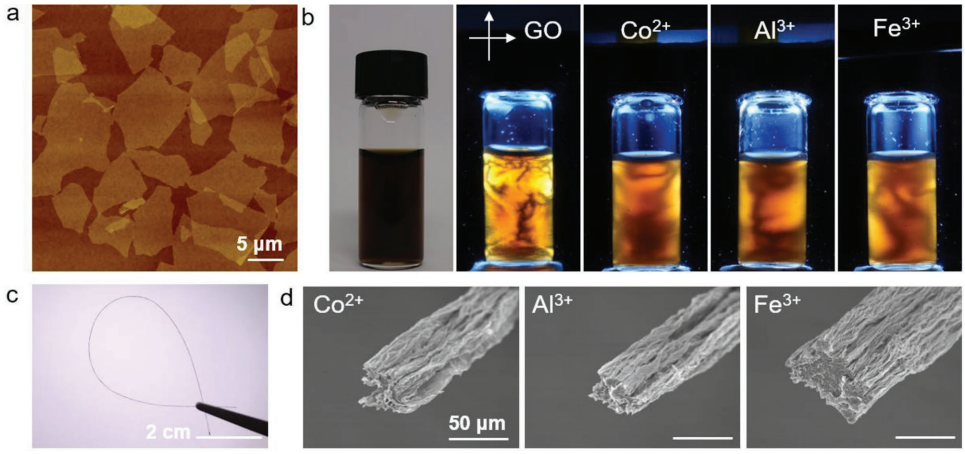


**Figure 1.** Observation of GO liquid crystal and fibers using each different coagulating salt. a) AFM image of single layer GO. b) Photographs of GO aqueous dispersion (1.0 mg $mL^{-1}$) and liquid crystalline dispersions between crossed polarizers. In last three vials, $20 \times 10^{-3}$ M $CaCl_2$, $AlCl_3$, $FeCl_3$ were mixed with GO, respectively, and left stational for a while. c) Photograph of GO fiber spun in coagulation bath containing $Co^{2+}$. d) SEM images of spun GO fibers with $Co^{2+}$, $Al^{3+}$, and $Fe^{3+}$, respectively.

so that, when tested, the properties of the GO fiber were due to the presence of the cations only. The collected GO fibers were washed with DIW to remove excess cations that were physically adsorbed to the GO sheets inside the gel. After being pulled from the washing bath, GO fibers were dried in air at room temperature.[10] Spun GO fibers proved to be strong and flexible when handled (Figure 1c). While fibers spun with trivalent salts are produced compact, the divalent spun fibers had a distorted appearance, as presented in Figure 1d. This difference suggests that the type of cation in coagulation is a major factor in the formation and properties of the GO fiber morphology.

The rheological behavior was used to examine the gelation behavior of the prepared mixture as shown in **Figure 2**. $Co^{2+}$, $Al^{3+}$, and $Fe^{3+}$ were used as binders due to their multivalency with the chloride anion. $Li^+$ was also tested for the comparison. It was reported that monovalent ions (e.g., $K^+$, $Li^+$, $Ag^+$) cannot lead to GO gelation, and flowed after vial inversion.[24] These results were similarly observed in the present work. Even when $100 \times 10^{-3}$ M LiCl was added to GO solution (5 mg $mL^{-1}$), the sol-gel transition of GO dispersion did not occur (Figure 2a,d). This indicates that monovalent ions are not suitable for binding of GO sheets. Ruoff and co-workers have shown that $Ca^{2+}$ and $Mg^{2+}$ enhance the mechanical properties of a layered GO paper by cross-linking.[21]

To compare the effect of divalent and trivalent cation on the gelation of GO, the gelation behavior was examined by the fluidity of the prepared mixture (Figure S1, Supporting Information). Due to the absence of attraction between GO sheets in DIW, the pristine GO solution flowed easily, whereas when mixed with divalent ($Co^{2+}$) and trivalent ($Al^{3+}$ and $Fe^{3+}$) cations, the GO formed hydrogels. Addition of cations in the GO dispersion leads to a network of GO sheets. Gelation occurred above different critical concentrations; $Co^{2+}$ ($15 \times 10^{-3}$ M), $Al^{3+}$ ($3 \times 10^{-3}$ M), and $Fe^{3+}$ ($3 \times 10^{-3}$ M) (Figure 2a,d).

Furthermore, the viscosities and storage modulus value of the trivalent hydrogel also exceeded the divalent hydrogels (Figure 2b,c). It implies that GO successfully developed 3D networked structures with both divalent and trivalent cations but the latter made stronger hydrogels. Higher viscosity and increased storage modulus of GO–cation hydrogels reveal that the di-/trivalent cations can coagulate GO sheets and cations in the hydrogel were well consolidated with GO sheets. The coordination of metal ions with hydroxyl and carboxyl groups on GO sheets is considered to be the main driving force for the assembly of GO sheets since multivalent metal ions usually have larger coordination stability constants than those of monovalent and divalent metals.[24] Therefore, rheological data (viscosity and storage modulus) reveal that trivalent cations have stronger cross-linking abilities and this leads to the gelation point at a low content level.

For summarization of the gelation behavior of GO, the phase diagram is presented in Figure 2d. The critical gelation concentrations of GO dispersion varied with each cation. The addition of the binder cation can increase the bonding force between GO sheets and consequently promote gelation. After the critical gelation concentration, a self-supporting structure fixed in the vial was observed. Interestingly, critical gelation concentration was strongly related to coordination number of metal cations.

Fibers spun with different diffusion of metal cations have different microstructures as highlighted in **Figure 3**. While microstructure control has been controlled by a variety of factors including dope constituents[25] and shear in the spinning orifice,[26] the diffusive effect of ionic binders has been less explored, even after attempts to control microstructure with coagulating medium.[27] However, on the basis of Fick's second law of diffusion, the rate of cation diffusion is strongly dependent on the diffusion coefficient; $Co^{2+}$ (1.08), $Al^{3+}$ (1.80), and $Fe^{3+}$ (1.36).[28–30] The spinning dope concentration was fixed for $450 \times 10^{-3}$ M for all GO fibers to exclude the previously reported effects. The morphologies of the fiber cross-section were reflected in the fiber properties, overall. While GO sheets are screened with cation binder, the diffusion rate changes the whole morphology of fiber. Since the diffusion in the core is slower than the shell, kinetics of each cation binder determines microstructure. For example, when the diffusion of cation is fast, structured robust core is formed relatively easily with

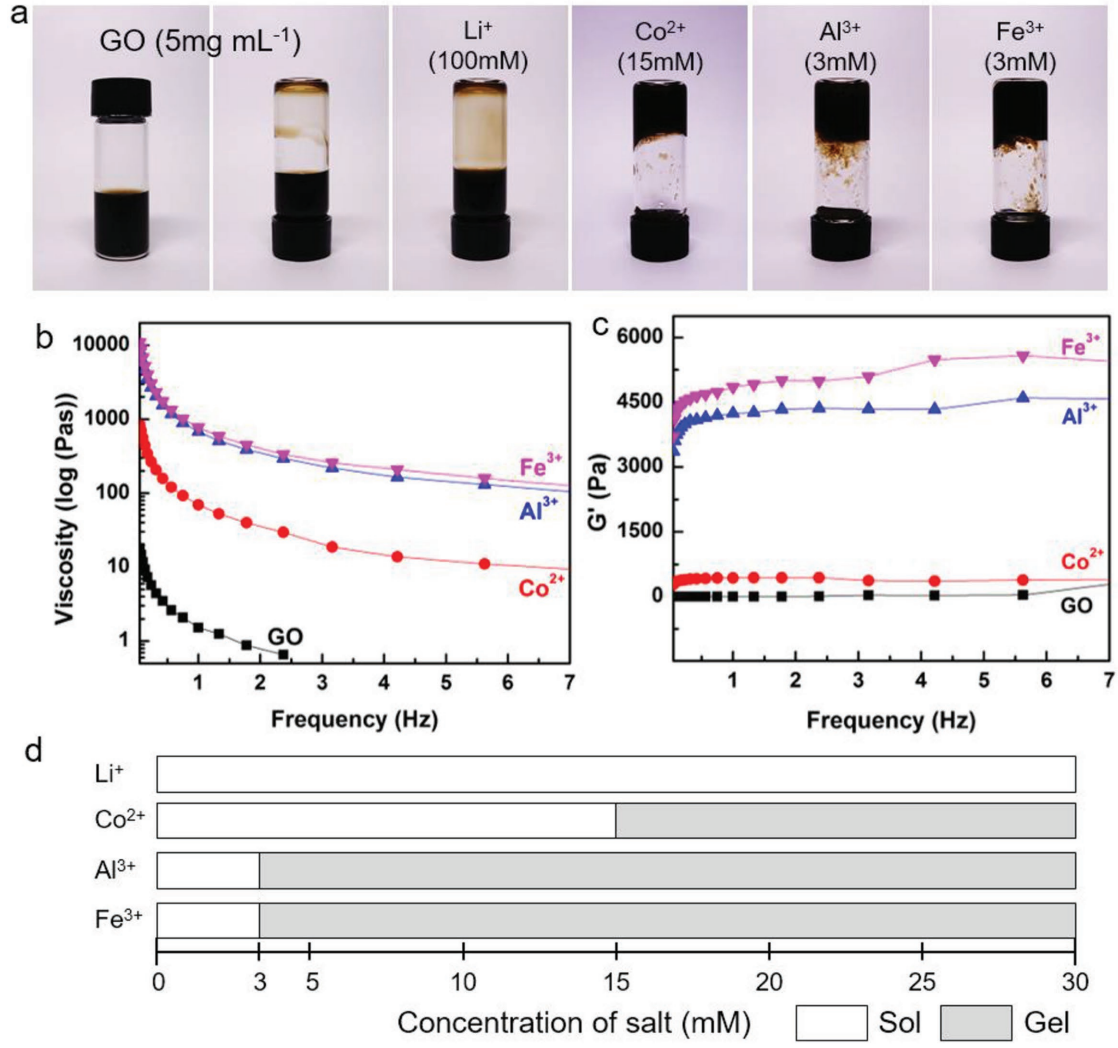


**Figure 2.** Gelation effect of di- and trivalent cations on GO dispersion. a) Photographs of the 5 mg mL$^{-1}$ GO solution and mixture with different cations: $Li^+$ ($100 \times 10^{-3}$ M LiCl); $Co^{2+}$ ($15 \times 10^{-3}$ M $CoCl_2$), $Al^{3+}$ ($3 \times 10^{-3}$ M $AlCl_3$), and $Fe^{3+}$ ($3 \times 10^{-3}$ M $FeCl_3$). b,c) Viscosities and storage modulus of GO–cation mixed gel presented in (a). d) Gelation phase diagram of GO dispersion mixed with monovalent ($Li^+$), divalent ($Co^{2+}$), and trivalent ($Al^{3+}$ and $Fe^{3+}$) cations.

reducing entropy effect. Therefore, the final morphology of the dried spun fiber is largely controlled by the cation diffusion rate. The structure of coagulated GO fibers with small core was uniform and compact due to the faster diffusion rate of cations.

For GO spinning, GO sheets are combined with the cations in the coagulation bath and bonded by electrostatic attractions (**Figure 4**a).[31] The *d*-spacing of GO sheets in GO fibers and pristine GO film was calculated from a distinct sharp (002) peak at around 10° of X-ray diffraction (XRD) pattern in Figure 4b using Bragg's law.[32] Dried GO fibers have different *d*-spacings according to the cation: GO film (8.08 Å), $Co^{2+}$ (8.79 Å), $Al^{3+}$ (9.01 Å), and $Fe^{3+}$ (9.51 Å), implying that the *d*-spacing of GO sheets in GO fibers increased with valence number of the cation. Figure 4c presents that the GO fibers' mechanical performance were improved when the cation valence number increased. Under tensile loading, the GO fiber demonstrates an elastic deformation. Trivalent ion coagulants were more effective for strengthening and stiffening the GO fiber than divalent ions for mechanical performance; about two times increase in strength and modulus when using $Fe^{3+}$ ions was observed. Furthermore, fracture toughness showed 23% increase (calculated by the area under the stress–strain curve). Mechanical properties including ultimate tensile strength, Young's modulus, and elongation at break are summarized in **Table 1.** The increased modulus and tensile strength is due to strong binding of GO sheets from edge to edge interaction. Increased distance between GO sheets induces the change of major interaction among GO sheets to edge to edge bonding, rather than basal plane interactions.[22] Therefore, the stronger binding interaction became more dominant than slippage of the oxygen group over the GO sheets. It brought a small strain ($Al^{3+}$: 0.69, $Fe^{3+}$: 0.62), resulting in increased stiffness (Young's modulus: $Al^{3+}$ (57 GPa), $Fe^{3+}$ (81 GPa)) (Figure 4c).[21] Strikingly, the structural superiority of the GO fiber with trivalent cations also improved the strength. The improvement could be attributed to the control of microstructure which changes chemical

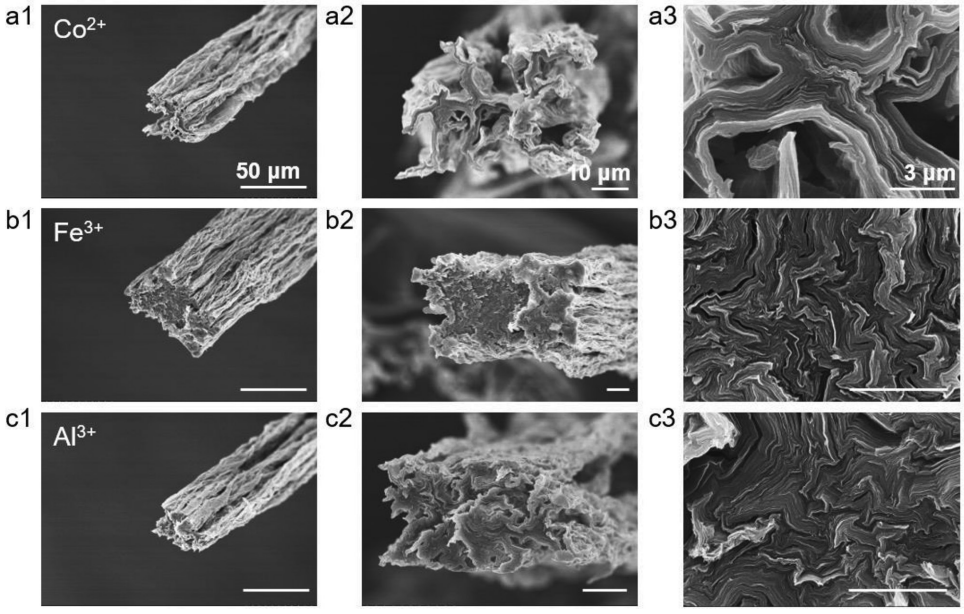


**Figure 3.** Cross-sectional SEM images of GO fibers at a low (column 1), medium (column 2), and high magnification (column 3) presenting morphological effects of various coagulating salts; a) $Co^{2+}$, b) $Fe^{3+}$, and c) $Al^{3+}$.

interlayer interactions of constituents, which ultimately affects mechanical performances.[4,33] Note that all cations have a different level of ionization energy, such as $Co^{2+}$ (1648 kJ $mol^{-1}$), $Al^{3+}$ (2745 kJ $mol^{-1}$), and $Fe^{3+}$ (2957 kJ $mol^{-1}$), allowing the high interlayer attractive force in the unique GO fiber structures to encompass the cations as binders.[34–37]

This report describes the role of trivalent metal cation binders as a coagulant for the fabrication of high performance GO fibers by wet spinning. The GO fiber with $Fe^{3+}$ exhibited superior mechanical performance, especially in terms of tensile strength (486 MPa), Young's modulus (81 GPa), and elongation at break (0.62%), which affects the resulting toughness (1.47 MJ $m^{-3}$). Trivalent cations were particularly advantageous for the diffusion and solidification of the fiber and led to improved strength and stiffness. The LC-GO fiber in the presence of trivalent metal cation binders led to a change of

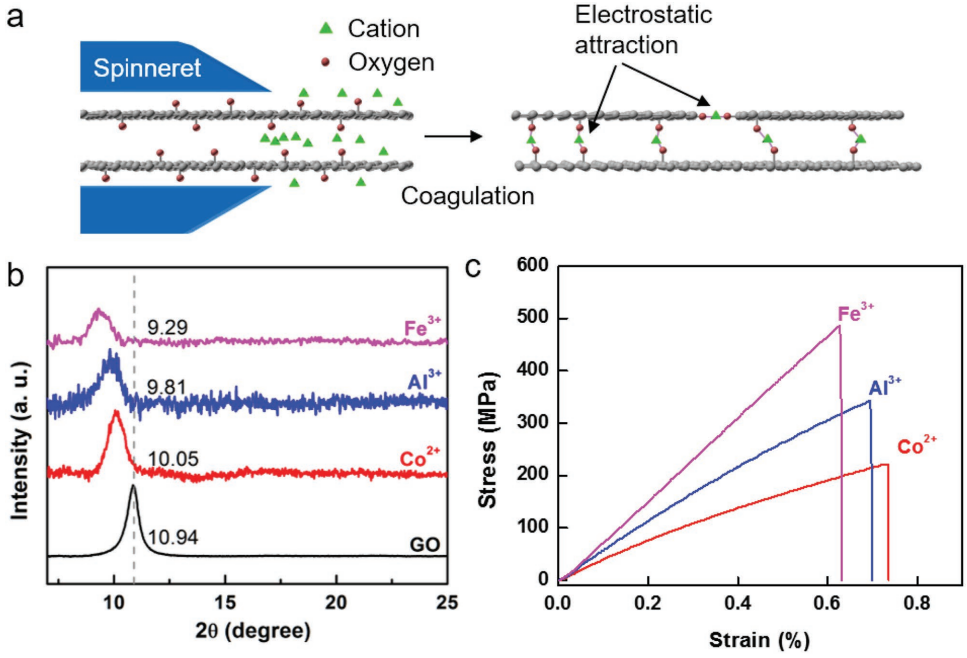


**Figure 4.** a) Schematic apparatus for spinning GO fiber. b) XRD patterns of GO film and GO fiber coagulated with different salts. c) Mechanical properties of spun GO fiber coagulated with various cation binders.

**Table 1.** Summary of the *d*-spacing, strength, stiffness, and elongation at break of spun GO fiber with different coagulating metal cation and GO film.

| | *d*-spacing [Å] | Ultimate tensile strength [MPa] | Young's modulus [GPa] | Elongation at break [%] | Toughness [MJ $m^{-3}$] |
|---|---|---|---|---|---|
| GO | 8.08 | – | – | – | – |
| $Co^{2+}$ | 8.79 | 221.22 | 37.1 | 0.74 | 1.20 |
| $Al^{3+}$ | 9.01 | 343.34 | 56.8 | 0.69 | 1.23 |
| $Fe^{3+}$ | 9.51 | 486.43 | 81.4 | 0.62 | 1.47 |

the *d*-spacing through the ionic interaction between GO sheets. Our approach to use metal cation binders in the coagulation step provides a straightforward strategy for the strong and high modulus GO fibers via the control of molecular interactions.

## Experimental Section

*Materials*: GO was prepared from graphite powder (Asbury Carbon) using the modified Hummers' method, according to the previous procedures.[21] Prepared GO powder was well dispersed in DIW.

*Gelation of GO*: To observe gelation behavior of GO, a set volume of GO dispersion (5 mg $mL^{-1}$) was mixed with different cations. The formation of the hydrogel was tested by a vial inversion method (glass vial with an inner diameter of 12 mm).

*Wet Spinning GO Fibers*: To obtain filamentous GO, GO dispersion was spun though a spinneret (diameter 400 µm) at a fixed velocity (10 mL $h^{-1}$) into the coagulation bath (cobalt(II) chloride, aluminum(III) chloride, and ferric(III) chloride, 0.45 M aqueous solution). Spun GO gel fibers in the bath were collected continuously on a reel. The resident time of GO fiber in the bath was ≈6 s. To compare the GO fiber properties according to changes in cations, spun GO fibers were not drafted. GO fibers were washed with DIW and dried at room temperature in a humidity controlled, home-made acrylic-box. The box was connected with fume hood and the relative humidity was kept at about 25%.

*Characterization*: Prepared GO sheets were observed via AFM (XE-70, Park Systems) in tapping mode. The optical birefringence of the prepared samples was characterized by observing the sample sealed in a vial or extruded gel located between crossed polarizers. The spun GO fibers were characterized using scanning electron microscopy (SEM, NOVA Nano SEM 450). Dynamic rheological properties were measured with MARS III rheometer (Thermo Scientific) under an oscillatory strain of 5% (cone-and-plate geometry, 20 mm in diameter, complementarity determining region of 0.5 radians, and a gap of 1 mm). XRD (D8 Advanced LynxEye) was carried out using Cu $K_\alpha$ radiation ($\lambda$ = 1.5418 Å). Tensile properties of GO fibers coagulated by different salts were investigated using universal testing machine (5966, Instron) equipped with a 10 N load cell operating at 2.5 mm $min^{-1}$ crosshead speed at gauge length of 25 mm by referring tensile measurement of single ultrafine fibers as reported before.[38,39] Fibers were loaded on a specific rectangular frame mentioned earlier. The mechanical strengths of graphene oxide fibers were calculated by the force divided by the cross-sectional area. For comparison, GO film was prepared using vacuum filtration and the *d*-spacing was also calculated with XRD characterization.

## Supporting Information

Supporting Information is available from the Wiley Online Library or from the author.

## Acknowledgements

The authors are grateful to Dr. Hannah S. Leese for her helpful discussion. The morphology of fiber (SEM) was analyzed on NOVA Nano SEM 450 installed at the Hanyang LINC Analytical Equipment Center (Seoul). This research was mainly supported by the Basic Science Research Program (NRF 2014R1A1A1008196) and the Nano Material Technology Development Program (NRF 2016M3A7B4905609) through the National Research Foundation of Korea funded by the Ministry of Science, ICT and Future. Also, it was partially supported by the MOTIE (Ministry of Trade, Industry & Energy) (10052027) and the KDRC (Korea Display Research Corp.).

Received: December 10, 2016
Revised: January 5, 2017
Published online: February 16, 2017

[1] J. E. Kim, T. H. Han, S. H. Lee, J. Y. Kim, C. W. Ahn, J. M. Yun, S. O. Kim, *Angew. Chem., Int. Ed.* **2011**, *50*, 3043.
[2] J. Y. Kim, S. O. Kim, *Nat. Mater.* **2014**, *13*, 325.
[3] Z. Xu, C. Gao, *ACS Nano* **2011**, *5*, 2908.
[4] F. Guo, F. Kim, T. H. Han, V. B. Shenoy, J. Huang, R. H. Hurt, *ACS Nano* **2011**, *5*, 8019.
[5] C. Xiang, C. C. Young, X. Wang, Z. Yan, C.-C. Hwang, G. Cerioti, J. Lin, J. Kono, M. Pasquali, J. M. Tour, *Adv. Mater.* **2013**, *25*, 4592.
[6] R. Jalili, S. H. Aboutalebi, D. Esrafilzadeh, R. L. Shepherd, J. Chen, S. Aminorroaya-Yamini, K. Konstantinov, A. I. Minett, J. M. Razal, G. G. Wallace, *Adv. Funct. Mater.* **2013**, *23*, 5345.
[7] Z. Xu, H. Sun, X. Zhao, C. Gao, *Adv. Mater.* **2013**, *25*, 188.
[8] J. Yu, Y.-G. Kim, D. Y. Kim, S. Lee, H.-I. Joh, S. M. Jo, *Macromol. Res.* **2015**, *23*, 601.
[9] Q. Zhang, L. Wang, Z. Wei, X. Wang, S. Long, J. Yang, *J. Polym. Sci., Part B: Polym. Phys.* **2012**, *50*, 1004.
[10] Z. Xu, C. Gao, *Nat. Commun.* **2011**, *2*, 571.
[11] T. H. Han, W. J. Lee, D. H. Lee, J. E. Kim, E.-Y. Choi, S. O. Kim, *Adv. Mater.* **2010**, *22*, 2060.
[12] K. W. Putz, O. C. Compton, M. J. Palmeri, S. T. Nguyen, L. C. Brinson, *Adv. Funct. Mater.* **2010**, *20*, 3322.
[13] H.-P. Cong, X.-C. Ren, P. Wang, S.-H. Yu, *Sci. Rep.* **2012**, *2*, 613.
[14] K. Yang, B. Chen, X. Zhu, B. Xing, *Environ. Sci. Technol.* **2016**, *50*, 11066.
[15] Y. Mo, X. Zhao, Y. Shen, *Desalination* **2016**. *399*, 40.
[16] B. Zheng, T. Huang, L. Kou, X. Zhao, K. Gopalsamy, C. Gao, *J. Mater. Chem. A* **2014**, *2*, 9736.
[17] T. H. Han, J. Kim, J. S. Park, C. B. Park, H. Ihee, S. O. Kim, *Adv. Mater.* **2007**, *19*, 3924.
[18] W. Song, I. A. Kinloch, A. H. Windle, *Science* **2003**, *302*, 1363.
[19] V. A. Davis, L. M. Ericson, A. N. G. Parra-Vasquez, H. Fan, Y. Wang, V. Prieto, J. A. Longoria, S. Ramesh, R. K. Saini, C. Kittrell, W. E. Billups, W. W. Adams, R. H. Hauge, R. E. Smalley, M. Pasquali, *Macromolecules* **2004**, *37*, 154.
[20] P. Borthakur, P. K. Boruah, N. Hussain, B. Sharma, M. R. Das, S. Matic, D. Reha, B. Minofar, *J. Phys. Chem. C* **2016**, *120*, 14088.
[21] S. Park, K.-S. Lee, G. Bozoklu, W. Cai, S. T. Nguyen, R. S. Ruoff, *ACS Nano* **2008**, *2*, 572.
[22] H. Park, T. H. Han, *Bull. Korean Chem. Soc.* **2013**, *34*, 3269.
[23] H. Huang, P. Chen, X. Zhang, Y. Lu, W. Zhan, *Small* **2013**, *9*, 1397.
[24] H. Bai, C. Li, X. Wang, G. Shi, *J. Phys. Chem. C* **2011**, *115*, 5545.
[25] Y. Ma, P. Li, J. W. Sedloff, X. Zhang, H. Zhang, J. Liu, *ACS Nano* **2015**, *9*, 1352.

  

[26] J. Sun, Y. Li, Q. Peng, S. Hou, D. Zou, Y. Shang, Y. Li, P. Li, Q. Du, Z. Wang, Y. Xia, L. Xia, X. Li, A. Cao, *ACS Nano* **2013**, *7*, 10225.
[27] S. H. Aboutalebi, R. Jalili, D. Esrafilzadeh, M. Salari, Z. Gholamvand, S. A. Yamini, K. Konstantinov, R. L. Shepherd, J. Chen, S. E. Moulton, P. C. Innis, A. I. Minett, J. M. Razal, G. G. Wallace, *ACS Nano* **2014**, *8*, 2456.
[28] A. C. F. Ribeiro, V. M. M. Lobo, J. J. S. Natividade, *J. Chem. Eng. Data* **2002**, *47*, 539.
[29] T. M. C. Faro, G. P. Thim, M. S. Skaf, *J. Chem. Phys.* **2010**, *132*, 114509.
[30] Z. C. Wu, Y. Awakura, S. Ando, H. Majima, *Mater. Trans., JIM* **1990**, *31*, 1065.
[31] H. Park, T. H. Han, *Macromol. Res.* **2014**, *22*, 809.
[32] L. Zhang, Y. D. Liu, H. J. Choi, *J. Mater. Chem.* **2011**, *21*, 6916.
[33] Z. Xu, Z. Liu, H. Sun, C. Gao, *Adv. Mater.* **2013**, *25*, 3249.
[34] R. Inskeep, *J. Inorg. Nucl. Chem.* **1962**, *24*, 763.
[35] Y. Li, H. Shimada, M. Sakairi, K. Shigyo, H. Takahashi, M. Seo, *J. Electrochem. Soc.* **1997**, *144*, 866.
[36] J. D. Rimstidt, D. J. Vaughan, *Geochim. Cosmochim. Acta* **2003**, *67*, 873.
[37] A. D. Arulsamy, *RSC Adv.* **2016**, *6*, 52082.
[38] T. J. Chuang, P. M. Anderson, M.-K. Wu, S. Hsieh, *Nanomechanics of Materials and Structures*, Springer, Dordrecht, The Netherlands **2006**.
[39] M. B. Bazbouz, G. K. Stylios, *J. Polym. Sci., Part B: Polym. Phys.* **2010**, *48*, 1719.